Available online at www.sciencedirect.com

ScienceDirect

Journal of Fluorine Chemistry 128 (2007) 219–223

www.elsevier.com/locate/fluor

# Microwave-assisted synthesis of spherical monodispersed magnesium fluoride

Mariusz Pietrowski [*], Maria Wojciechowska

*Adam Mickiewicz University, Faculty of Chemistry, 60-780 Poznań, Grunwaldzka 6, Poland*

Received 13 September 2006; received in revised form 7 December 2006; accepted 15 December 2006
Available online 20 December 2006

## Abstract

Spherical monodispersed magnesium fluoride has been obtained using the microwave-assisted precipitation technique from magnesium nitrate and ammonium fluoride solutions. Studies aimed at optimizing synthesis conditions from the point of view of preparing spherical $MgF_2$ particles of possibly high monodispersity were performed. Spherical $MgF_2$ particles of 0.25–0.36 μm in diameter have been obtained with relative standard deviation from the average value ranging from 7 to 15%. It has been established that a certain optimal range of $Mg(NO_3)_2$ and $NH_4F$ concentrations exists that enables a highly monodispersed $MgF_2$ to be prepared. The range is narrow (0.01–0.03 mol dm$^{-3}$) for both precursors. Spherical $MgF_2$ particles have been characterized by SEM, XRD, DTG/DTA and FTIR techniques.

*Keywords:* Monodispersed magnesium fluoride; Spherical magnesium fluoride; Microwave-assisted synthesis; $MgF_2$

## 1. Introduction

The fascination with monodispersed colloids began from experiments carried out almost one and a half centuries ago by Faraday, who prepared gold sols and described their glistening colours that were particle-size dependent [1]. At first homogeneously dispersed matter attracted the attention of academic circles only and concerned studies of its physical and chemical properties as well as their relation with size and shape of particles. Now it is possible to prepare monodispersed materials from a few nanometers to a few micrometers in diameter. Many compounds, for example $SiO_2$ [2,3], $TiO_2$ [4–7], $ZrO_2$ [8,9], sulfides [10–12], carbonates [13–15] and halides [16,17] have been synthesized in the form of monodispersed particles. Such materials have found application in ceramics, manufacture of pigments, manufacture of electronic data carriers, medical diagnostics and catalysis.

One of the halides, for which attempts have been made to obtain it in the form of spherical particles, is magnesium fluoride. It crystallizes in the rutile structure. The coordination surrounding of magnesium ions has a distorted octahedral shape, where the Mg–F distances are 1.94 Å for four fluorine ions and 1.99 Å for the other two [18]. $MgF_2$ shows good thermal stability and significant hardness. It is an insulator with a broad band gap. Magnesium fluoride is used extensively in optical thin films [19–23], for example, as anti-reflective coatings on glasses and as rutile seed for pigment applications [24] and for composite optical filters with titania [25]. It was also reported that magnesium fluoride, which played the role of a support for a number of oxide [26,27], metallic [28] and sulfide [29] phases, enabled syntheses of catalysts active for such reactions as decomposition and reduction of nitrogen oxides [30], hydrodechlorination of chlorofluorocarbons (CFC) [31] and hydrodesulfurization of thiophene [32,33].

In conventional thermal processing, energy is transferred to the material through convection, conduction, and radiation of heat from the surfaces of the material which results in temperature gradient formation. In contrast, microwave heating leads to the direct interaction between microwaves and materials and this fact enables an uniform and fast heating of a sample. This difference can result in many potential advantages for microwaves in processing of materials. Therefore microwave-assisted synthesis has been applied widely in various fields such as molecular sieve preparation, the preparation of inorganic complexes and oxides, organic reactions, plasma chemistry, analytical chemistry and catalysis [34,35].

---

[*] Corresponding author. Tel.: +48 61 8291470; fax: +48 61 8658008.
*E-mail address:* mariop@amu.edu.pl (M. Pietrowski).

0022-1139/$ – see front matter © 2007 Elsevier B.V. All rights reserved.
doi:10.1016/j.jfluchem.2006.12.009

In this study, synthesis of spherical magnesium fluoride particles was performed by means of $MgF_2$ precipitation from solutions of $NH_4F$ and $Mg(NO_3)_2$, heated in a conventional kitchen microwave oven. The approach was aimed at initiating the reaction over the entire volume of the solution, which should result in spherical $MgF_2$ particles of high monodispersity. The formation of spherical $MgF_2$ particles has been previously reported by Matijević and co-workers [16]. They heated the solution of $MgCl_2$ and NaF in a conventional way. In our study, the precursors of magnesium fluoride were $Mg(NO_3)_2$ and $NH_4F$. During thermal treatment of the precipitated $MgF_2$ the impurities such as nitrate and ammonium ions decompose which results in the formation of chemically pure magnesium fluoride. This fact is of importance to catalytic applications of $MgF_2$, because even trace impurities can change significantly its catalytic properties.

## 2. Results and discussion

The effect of magnesium nitrate and ammonium fluoride concentrations (Table 1) on the shape of precipitated particles was studied and results were presented in Fig. 1. Spherical magnesium fluoride particles can be prepared only in a strictly specified precursor concentration range: 0.006–0.03 mol $dm^{-3}$ for $Mg(NO_3)_2$ and 0.01–0.09 mol $dm^{-3}$ for $NH_4F$. However, F:Mg molar ratio does not exert any significant effect on the shape of the precipitates formed. Even if one of the precursors is used at a higher concentration, a gel is formed that gives amorphous $MgF_2$. SEM micrographs of the $MgF_2$ precipitates obtained are presented in Fig. 2, where pictures of spherical $MgF_2$ particles (sample A) as well as amorphous sample D are shown.

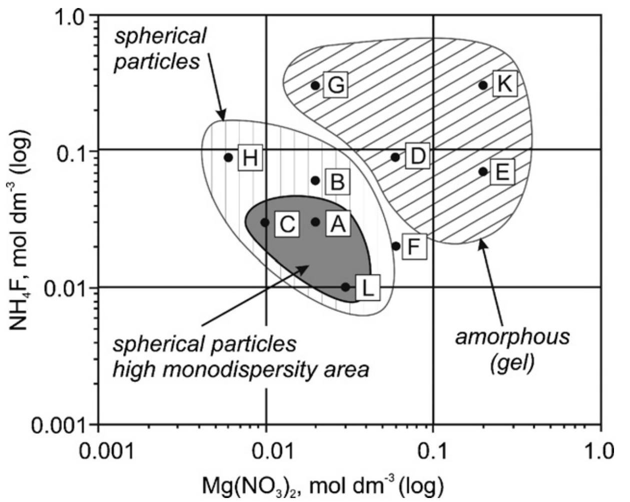

Fig. 1. The effect of $Mg(NO_3)_2$ and $NH_4F$ concentrations on properties of precipitates obtained by exposing aqueous solutions to microwave radiation.

From the SEM micrographs, average size of spherical magnesium fluoride particles ($d_{AV}$) and average standard deviation of particle size (S.D.) were calculated—Table 1. The average size of spherical magnesium fluoride particles falls in the range 0.25–0.36 μm and the average standard deviation of particle size, that is a measure of monodispersity, ranges from 7 to 15%. There was no clear dependence of the particle size on the precursor concentration, although such a dependence (an increase in $MgF_2$ particle size with decreasing NaF concentration) was observed by Matijević and co-workers in the case of $MgF_2$ preparation from $MgCl_2$ and NaF using the conventional way of heating in a furnace [16]. It seems reasonable to suppose that the lack of the dependence arise from completely different preparation conditions and precursors of $Mg^{2+}$ and $F^{-}$ ions. The highest monodispersity was found in samples A, C and L (Fig. 1). The best monodispersity area is located in a very narrow range of concentration of magnesium nitrate and ammonium fluoride 0.01–0.03 mol $dm^{-3}$ (Fig. 1 and Table 1).

The magnesium fluoride sample A showing the highest monodispersity, has X-ray patterns typical of crystalline rutile $MgF_2$ (Fig. 3). No reflections originating from other crystalline phases were observed, which proves thorough washing off of unreacted precursors and high purity of $MgF_2$ obtained. The X-ray spectra show a gradual increase in the sample crystallinity as the calcination temperature increases, as shown by higher

Table 1
Conditions of magnesium fluoride preparation[a], average spherical particle diameter and its relative standard deviation

| Sample code | Precursor concentration (mol $dm^{-3}$) | | F:Mg molar ratio | $d_{AV}$[b] (μm) | S.D.[c] (%) |
|---|---|---|---|---|---|
| | $NH_4F$ | $Mg(NO_3)_2$ | | | |
| *A* | *0.03* | *0.02* | *3:1* | *0.36* | *7* |
| B | 0.06 | 0.02 | 6:1 | 0.25 | 15 |
| *C* | *0.03* | *0.01* | *6:1* | *0.31* | *9* |
| D | 0.09 | 0.06 | 3:1 | Amorphous (gel) | – |
| E | 0.07 | 0.20 | 2:1 | Amorphous (gel) | – |
| F | 0.02 | 0.06 | 1.33:1 | 0.29 spherical and nonspherical | 15 |
| G | 0.30 | 0.02 | 30:1 | Amorphous (gel) | – |
| H | 0.09 | 0.006 | 30:1 | 0.35 | 15 |
| K | 0.30 | 0.20 | 3:1 | Amorphous (gel) | – |
| *L* | *0.01* | *0.03* | *1.33:1* | *0.30* | *8* |

[a] The preparation conditions resulting in the highest particle monodispersity are italicized.

[b] Average particle diameter.

[c] Relative standard deviation.

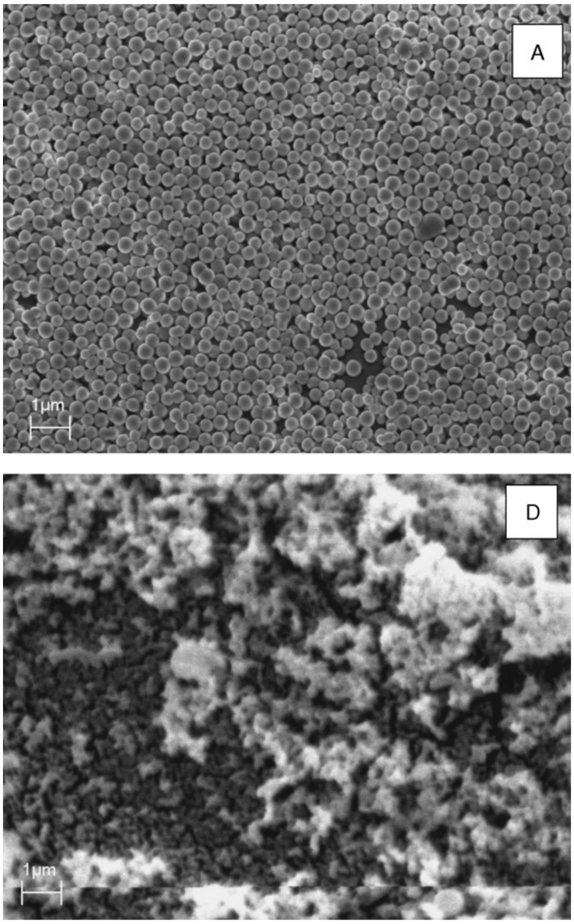

Fig. 2. Scanning electron micrographs of $MgF_2$ particles: spherical (sample A) and amorphous ones (sample D).

intensity of reflections and their clear narrowing (Fig. 3). From three reflections originating from the same family of planes (1 1 0), (2 2 0) and (3 3 0), using the Hall method, sizes of crystallites that form the mosaic structure of $MgF_2$ were calculated. Crystallite sizes clearly grow with increasing calcination temperature—from 22 nm when heated at 280 °C to 62 nm when heated at 380 °C (Table 2). This growth of crystallite size is accompanied by a reduction in $MgF_2$ specific surface area—from 21 to 8 $m^2\ g^{-1}$ (Table 2). Such an effect is not a surprise, because higher calcination temperature results in sintering of narrow pores and recrystallization of samples.

Thermogravimetric analysis indicates that mass loss of magnesium fluoride sample A in the range 20–650 °C is 11.7%

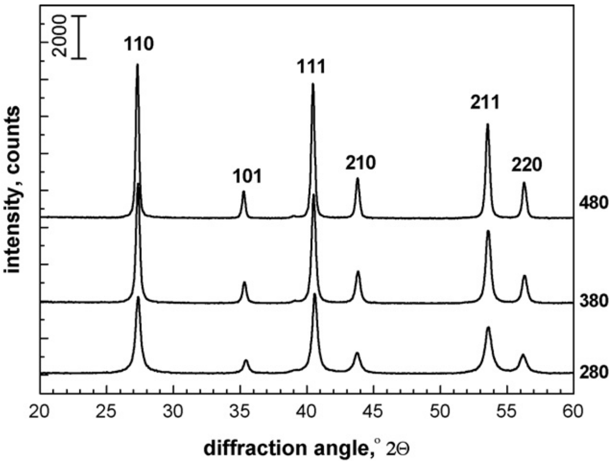

Fig. 3. X-ray diffraction patterns of spherical $MgF_2$ particles (sample A) calcined at 280, 380 and 480 °C.

Table 2

The effect of calcination temperature on the average crystallite size and BET surface area of $MgF_2$ spherical particles—sample A

| Calcination temperature (°C) | Surface area ($m^2\ g^{-1}$) | Crystallite size (nm) |
|---|---|---|
| 280 | 21 | 22 |
| 380 | 16 | 47 |
| 480 | 8 | 62 |

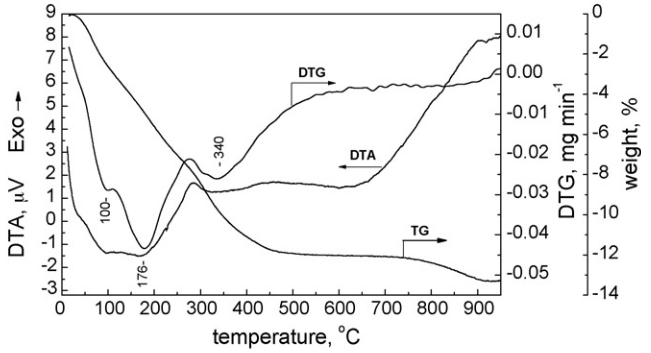

Fig. 4. Thermogravimetric curve (TG), its first derivative (DTG) and differential thermal analysis (DTA) curve of $MgF_2$ spherical particles (sample A).

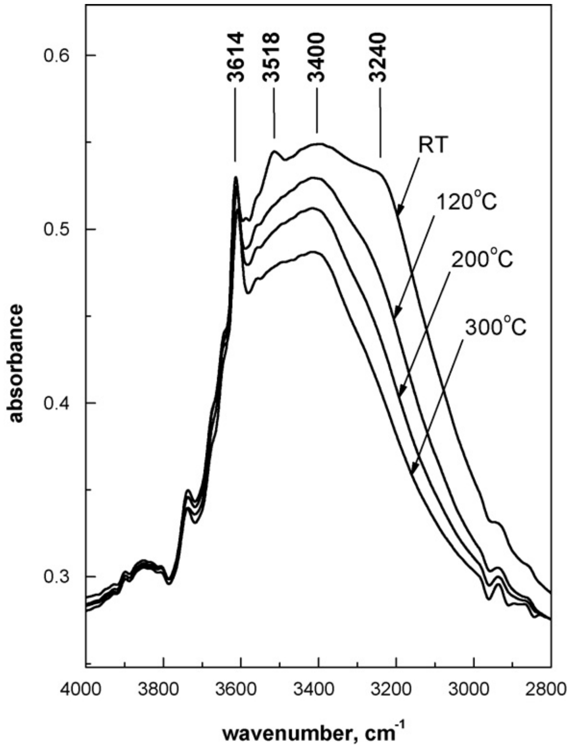

Fig. 5. FTIR spectra of $MgF_2$ spherical sample A evacuated for 30 min at different temperatures.

(Fig. 4). It proceeds by three stages with maxima at 100, 176 and 340 °C, which are accompanied by endothermic effects in the DTA curve. The first mass loss (1.4%) should be ascribed to desorption of physically adsorbed water; the next two peaks (mass loss of 5.5 and 4.8%, respectively) originate from dehydroxylation of the $MgF_2$ surface. This is confirmed by FTIR spectra in the –OH stretching region (Fig. 5). After outgassing at room temperature, there are four strong bands originating from different types of hydroxyl groups. They differ in their susceptibility to dehydroxylation, which is reflected by differences in the reduction of band intensity as a function of temperature. The most stable are the OH groups responsible for the band at 3614 $cm^{-1}$; this band remains almost unchanged even after evacuation at 300 °C. Intensities of the other bands located at 3518, 3400 and 3240 $cm^{-1}$ decrease with increasing outgassing temperature.

## 3. Conclusions

Spherical $MgF_2$ particles of 0.25–0.36 μm in diameter and high monodispersity (S.D. = 7–15%) has been obtained by the precipitation reaction between magnesium nitrate and ammonium fluoride. Spherical magnesium fluoride particles can be prepared only when using precursors in a strictly specified concentration range: 0.006–0.03 mol $dm^{-3}$ for $Mg(NO_3)_2$ and 0.01–0.09 mol $dm^{-3}$ for $NH_4F$. At higher concentrations of any of the precursors, a gel is obtained that results in amorphous $MgF_2$. No correlation has been observed between the particle size and the precursor concentration as well as between the particle size and the F:Mg molar ratio. The spherical $MgF_2$ is clearly crystalline and has the rutile type structure. The crystallinity increases with sample calcination temperature, which results in the growth of size of mosaic structure-making crystallites from 22 to 62 nm after calcination at 280 and 480 °C, respectively. The increase in crystallinity is accompanied by a reduction in surface area from 21 to 8 $m^2\,g^{-1}$. During heating of spherical $MgF_2$, dehydration followed by dehydroxylation occur, which are reflected by clear endothermic effects in DTA curves and a decrease in intensities of bands originated from hydroxyl groups in FTIR spectra. Total loss of mass caused by dehydration and dehydroxylation was 11.7%.

## 4. Experimental

### 4.1. Preparation of $MgF_2$ particles

All reagents were of analytic purity. Magnesium fluoride was prepared according to the reaction equation:

$$Mg(NO_3)_2 + NH_4F \rightarrow MgF_2 + NH_4NO_3$$

by heating of aqueous solution of $NH_4F$ and $Mg(NO_3)_2$ using a regular kitchen microwave oven equipped with a magnetron of 2.45 GHz frequency. During heating, the solution has been intensively stirred with the use of a mechanical stirrer introduced through a hole in the upper shield of the oven. Cold solutions of ammonium fluoride and magnesium nitrate (total volume of 150 $cm^3$) with appropriate concentrations were mixed in a beaker and then immediately transferred to the microwave oven, where the combined solution was heated to boiling within 20 s with intensive stirring. After removal from the microwave oven, the sample was cooled down to room temperature (~10 s) by pouring the reaction mixture to 300 $cm^3$ of cold water.

The solids were separated by centrifugation, rinsed several times with distilled water, and finally the powder was dried in air at 80 °C for 24 h. In order to optimize the preparation of $MgF_2$ spherical particles of possibly narrowest size range, the precipitation of $MgF_2$ from a number of solutions of different concentrations and different molar ratios of magnesium and fluorine precursors, was investigated. Sample codes and precursor concentrations are listed in Table 1.

Concentrations of $NH_4F$ ranged from 0.01 to 0.30 mol $dm^{-3}$ and those of $Mg(NO_3)_2$ from 0.006 to 0.20 mol $dm^{-3}$. The preparation was carried out for F:Mg molar ratios equal to 1.33:1, 2:1, 3:1, 6:1 and 30:1.

### 4.2. Scanning electron microscopy (SEM)

SEM micrographs of $MgF_2$ samples were taken on a scanning electron microscope Philips SEM 515. On the ground of the micrographs, average size of spherical magnesium fluoride particles ($d_{AV}$) and average standard deviation of particle size (S.D.) were calculated.

### 4.3. X-ray diffraction

XRD experiments were performed using a Philips PW1050 diffractometer equipped with Cu Kα source and Ni filter in the range of 3–152° $2\theta$. On the basis of (1 1 0), (2 2 0) and (3 3 0) reflections, the crystallite size was measured by using the Hall method [36].

### 4.4. Surface area and pore size distribution

The low temperature adsorption and desorption of nitrogen were measured on an ASAP 2010 sorptometer manufactured by Micromeritics. Specific surface area was determined by the BET method.

### 4.5. Thermal analyses

Thermogravimetric analysis (TG) and differential thermal analysis (DTA) were carried out in the temperature range of 30–1000 °C using a differential thermoanalyzer Netzsch STA C 3F, equipped with a TG measurement unit. The experiments were performed under nitrogen flow (99.995% purity) and temperature increase rate of 8 K $min^{-1}$.

### 4.6. FTIR spectroscopy

FTIR experiments were carried out using a BIORAD spectrometer, model FTS 3000MX. The spectra were recorded in the range 4000–2800 $cm^{-1}$. $MgF_2$ wafers (4 mg $cm^{-2}$) were placed in a glass cell equipped with KRS-5 windows. Such a cell enables the obtain infrared spectra of samples heated *in situ* to 300 °C. The samples were evacuated to reach the vacuum of $10^{-4}$ Pa.

## References

[1] M. Faraday, Philos. Trans. Roy. Soc. Lond. 147 (1857) 145–153.
[2] S.K. Park, K.D. Kim, Colloids Surf. A 197 (2002) 7–17.
[3] L.M. Yang, Y.J. Wang, Y.W. Sun, G.S. Luo, Y.Y. Dai, J. Colloid Interf. Sci. 299 (2006) 823–830.
[4] M. Keshmiri, T. Troczynski, J. Non-Cryst. Solids 311 (2002) 89–92.
[5] H.K. Park, Y.T. Moon, D.K. Kim, C.H. Kim, J. Am. Ceram. Soc. 79 (1996) 2727–2732.
[6] H.S. Potdar, S.B. Deshpande, S. Mayadevi, P.A. Joy, S.K. Date, Indian J. Chem. A 38 (1999) 468–472.
[7] E.A. Barringer, H.K. Bowen, Langmuir 1 (1985) 414–420.
[8] J. Wang, W. Li, L. Gao, J. Mater. Sci. Lett. 19 (2000) 159–161.
[9] O. VanCantfort, B. Michaux, R. Pirard, J.P. Pirard, A.J. Lecloux, J. Sol-Gel Sci. Technol. 8 (1997) 207–211.
[10] S. Libert, V. Gorshkov, V. Privman, D. Goia, E. Matijević, Adv. Colloid Interf. Sci. 100 (2003) 169–183.
[11] K. Okuyama, I.W. Lenggoro, N. Tagami, S. Tamaki, N. Tohge, J. Mater. Sci. 32 (1997) 1229–1237.
[12] Z. Hu, L. Li, X. Zhou, X. Fu, G. Gu, J. Colloid Interf. Sci. 294 (2006) 328–333.
[13] M.L. Panchula, M. Akinc, J. Eur. Ceram. Soc. 16 (1996) 833–841.
[14] J.G. Yu, M. Lei, B. Cheng, Mater. Chem Phys. 88 (2004) 1–4.
[15] P. Jeevanandam, Y. Koltypin, O. Palchik, A. Gedanken, J. Mater. Chem. 11 (2001) 869–873.
[16] W.P. Hsu, Q. Zhong, E. Matijević, J. Colloid Interf. Sci. 181 (1996) 142–148.
[17] J.L. Lemyre, A.M. Ritcey, Chem. Mater. 17 (2005) 3040–3043.
[18] A.F. Wells, Structural Inorganic Chemistry, 3rd ed., Clarendon Press, Oxford, 1962, p. 337.
[19] S. Fujihara, M. Tada, T. Kimura, Thin Solid Films 304 (1997) 252–255.
[20] N. Bazin, J.E. Andrew, H.A. McInnes, J. Sol-Gel Sci. Technol. 13 (1998) 757–761.
[21] P.A. Sermon, R. Badheka, J. Sol-Gel Sci. Technol. 32 (2004) 149–153.
[22] J.K. Murthy, U. Gross, S. Rudiger, E. Kemnitz, J.M. Winfield, J. Solid State Chem. 179 (2006) 739–746.
[23] A.A. Rywak, J.M. Burlitch, Chem. Mater. 8 (1996) 60–67.
[24] E. Matijević, P.W. Hsu, M.R. Kuehnle, US Patent 5,248,556 (1993).
[25] E. Širbegović, M. Čevo, I. Tucak, Vacuum 43 (1992) 723–725.
[26] M. Wojciechowska, J. Goslar, W. Kania, M. Pietrowski, J. Fluorine Chem. 91 (1998) 141–145.
[27] M. Wojciechowska, J. Goslar, M. Pietrowski, Mol. Phys. Rep. 18/19 (1997) 143–147.
[28] M. Wojciechowska, S. Lomnicki, M. Pietrowski, Catal. Lett. 46 (1997) 63–69.
[29] M. Wojciechowska, M. Pietrowski, B. Czajka, Catal. Today 65 (2001) 349–353.
[30] M. Wojcichowska, M. Zieliński, M. Pietrowski, Catal. Today 90 (2004) 35–38.
[31] A. Malinowski, W. Juszczyk, J. Pielaszek, M. Bonarowska, M. Wojciechowska, Z. Karpiński, Chem. Commun. 8 (1999) 685–686.
[32] M. Wojciechowska, M. Pietrowski, B. Czajka, S. Lomnicki, Catal. Lett. 87 (2003) 153–157.
[33] M. Wojciechowska, M. Pietrowski, S. Lomnicki, Chem. Commun. 5 (1999) 463–464.
[34] E.T. Thostenson, T.-W. Chou, Composites Part A 30 (1999) 1055–1071.
[35] A. Gedanken, Ultrason. Sonochem. 11 (2004) 47–55.
[36] A. Taylor, X-ray Metallography, John Willey and Sons, New York, London, 1961, p. 778.